



# Pulsed electrochemical deposition of calcium phosphate coatings for biomedical applications

F. Lissandrello & L. Magagnin

To cite this article: F. Lissandrello & L. Magagnin (2023): Pulsed electrochemical deposition of calcium phosphate coatings for biomedical applications, Transactions of the IMF, DOI: [10.1080/00202967.2023.2207334](https://doi.org/10.1080/00202967.2023.2207334)

To link to this article: <https://doi.org/10.1080/00202967.2023.2207334>



Published online: 11 May 2023.



Submit your article to this journal [↗](#)



Article views: 16



View related articles [↗](#)



View Crossmark data [↗](#)

# Pulsed electrochemical deposition of calcium phosphate coatings for biomedical applications

F. Lissandrello  and L. Magagnin 

Dipartimento di Chimica, Materiali e Ingegneria Chimica 'Giulio Natta', Politecnico di Milano, Milano, Italy

## ABSTRACT

Calcium phosphate coatings have been widely used in orthopaedic and dental implants due to their excellent bioactivity and ability to promote formation of new bone tissue. Among the techniques used to manufacture these materials, electrochemical deposition has emerged as a promising method due to several benefits, such as improved compositional control, coating uniformity, versatility, and low cost. Moreover, the use of a pulsed current has proved to be an effective strategy to overcome electrochemical deposition's major shortcomings. Herein, we provide an overview of the electrochemical deposition method, highlighting the benefits of the use of a pulsed current, as well as discussing the recent advances in the field. Overall, pulsed electrochemical deposition represents a promising approach for the production of high quality calcium phosphate coatings tailored for orthopaedic and dental implants.

## KEYWORDS

Calcium phosphate; electrochemical deposition; electrodeposition; pulsed current

## Introduction

Calcium phosphate is a biocompatible and bioactive ceramic material that is often used in medical implants for bone repair. The presence of calcium phosphate in medical implants actively promotes bone regeneration while ensuring excellent adhesion between the device and the newly formed tissue.<sup>1,2</sup>

Owing to its poor mechanical properties, calcium phosphate is never used as a standalone material; instead, it is often employed as a coating on biocompatible metals, ranging from the state-of-the-art titanium and its alloys<sup>3</sup> to the more recently introduced biodegradable alloys based on magnesium,<sup>4,5</sup> zinc,<sup>6,7</sup> or iron.<sup>8,9</sup> While these metals are able to provide the required mechanical support and are adequately biocompatible, they are not intrinsically bioactive – i.e. they do not cause the insurgence of adversary effects while in contact with a biological system, but at the same time they do not interact significantly with the bone tissue forming around them.<sup>10</sup> It has been reported that poor bioactivity induces the formation of a fibrous membrane that surrounds the implant without a cohesive interface between the two.<sup>11</sup> Ultimately this might lead to premature failure of the anchoring points of the growing bone tissue, detachment of the implant and the requirement of a revision surgery.<sup>12</sup> Calcium phosphate coatings are therefore introduced to provide appropriate surface characteristics, such as morphology, roughness, porosity and, most importantly, chemical composition. Moreover, in the case of biodegradable alloys, a calcium phosphate coating serves the additional purpose of tuning the corrosion rate of the metal, ensuring controlled degradation of the implant.<sup>13</sup>

Calcium phosphate coatings have been synthesised with a wide array of deposition methods, with the main one being plasma spraying.<sup>14</sup> With this technique it's possible to fabricate coatings with adequate thickness and superficial properties, while still maintaining high throughput and moderately low cost. These features combined made plasma spraying the most widespread technique for many decades. Plasma

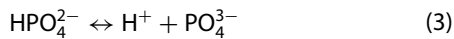
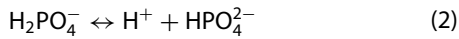
spraying, however, is far from being an ideal fabrication method; major shortcomings of this technique include the high temperature and fast cooling rates required for the process, which often lead to difficulties in control of the coating composition.<sup>15</sup> Moreover, plasma spraying is a so called line-of-sight technique, meaning that only the surfaces which are directly exposed to the plasma can be coated. This aspect imposes a challenge when coating complex geometries, especially when hollow features are present.<sup>16</sup> Therefore, a significant effort has been devoted to find an alternative deposition technique. Some examples include, but are not limited to, magnetron sputtering,<sup>17,18</sup> sol-gel,<sup>19,20</sup> dip coating,<sup>21–23</sup> pulsed laser deposition,<sup>24</sup> electrophoresis,<sup>25–27</sup> and electrochemical deposition.<sup>12,28,29</sup> Among these methods, electrochemical deposition has gained meaningful attention due to the low operating temperature, improved composition control, low cost, and possibility of introducing doping elements and molecules with relative ease.

In electrochemical deposition the samples are connected to the cathode of a two-electrode cell containing an aqueous solution of the calcium and phosphate precursors. By applying a cathodic polarisation to the sample, it is possible to trigger a series of chemical reactions which ultimately end up with the precipitation of the calcium phosphates on its surface. An inert anode is also present in the electrochemical cell to close the circuit. The polarisation applied can be either constant or pulsed; in this review the electrochemical method will be initially described, showing how the different initial parameters affect the coating final features. Then an effort will be made to highlight the advantages of the pulsed method over the continuous one.

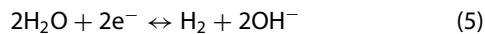
## The deposition process and resulting phases

The foundation of this process is the dissociation of phosphoric acid to generate  $\text{HPO}_4^{2-}$  and  $\text{PO}_4^{3-}$  ions *in situ*. Since

phosphoric acid is a weak triprotic acid, it will undergo proton exchange reactions at different pH:



Reactions 1, 2 and 3 have a pKa of 2.14, 7.21, and 12.34 respectively and dictate which is the most stable phosphate species as a function of pH.<sup>30</sup> In electrochemical calcium phosphate deposition, the pH of the electrolyte typically ranges between 4 and 5, with the majority of phosphate species being the dihydrogen phosphate ion,  $\text{H}_2\text{PO}_4^-$ . The core mechanism in the electrochemical calcium phosphate coating formation is to introduce an increase of pH confined at the surface of the cathode, so that the equilibrium is shifted towards the  $\text{HPO}_4^{2-}$  and  $\text{PO}_4^{3-}$  ions. When this condition is met, calcium phosphate precipitation spontaneously occurs on the cathode surface, due to the low solubility of the secondary and tertiary phosphate species. The shift in pH is obtained by applying a cathodic polarisation to the uncoated bone implant, allowing hydrogen evolution to take place with two different possible pathways:



Reaction 4 is favoured at acidic pH, while reaction 5 is more common in neutral or alkaline pH. Regardless of the actual pathway, the outcome of these reactions is always an increase in pH, either by consumption of free  $\text{H}^+$  ions or by production of  $\text{OH}^-$  ions. In general, hydrogen evolution is not the only redox reaction contributing to the desired pH increase and later some additional mechanisms will be presented. If the pH at the cathode interface is sufficiently high,  $\text{HPO}_4^{2-}$  and  $\text{PO}_4^{3-}$  species will be formed and solid calcium phosphates will precipitate due to their low solubility. Table 1 provides an overview of the most common phases obtained with calcium phosphate electrochemical deposition as well as their solubility.

The composition of the coatings produced with the electrochemical method varies strongly with the adopted parameters. Of these phases, hydroxyapatite (HA) is the most researched in literature, due to its low solubility and similar structure to bone and teeth mineral. Nevertheless, the actual composition of human bones is more similar to calcium-deficient apatite (CDA) with traces of secondary ions, such as  $\text{CO}_3^-$ ,  $\text{Mg}^{2+}$  and so on.<sup>32</sup> Other crystalline phases such as dicalcium phosphate dihydrate (DCPD) and octacalcium phosphate (OCP), as well as amorphous calcium phosphate (ACP), are less studied due to their high solubility which could hinder their application in medical devices. Still, this aspect can also be exploited to engineer the release of beneficial doping elements over time<sup>33</sup> or to induce the formation of HA and CDA *in vivo*.<sup>34</sup>

In 2009 Shaolin Chen *et al.* developed a model that could correlate the parameters of a continuous current electrochemical deposition with the crystalline phases obtained.<sup>35</sup> The starting point of their work, which is based on thermodynamics and kinetics of crystallisation, is the correlation between the  $\text{OH}^-$  concentration at the interface ( $C_{(t)}$ ) and deposition parameters, such as current density ( $j_0$ ), time ( $t$ )

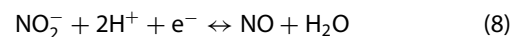
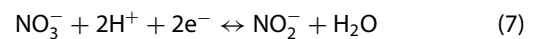
and initial concentration ( $C_0$ ):

$$C_{(t)} = C_0 + \frac{2j_0\sqrt{\pi Dt}}{nF\pi D} \quad (6)$$

where  $D$  is the diffusion coefficient of  $\text{OH}^-$  ions ( $D = 5.28 \cdot 10^{-5} \text{ cm}^2 \text{ s}^{-1}$ ). From the hydroxyl ion concentration, it is then possible to estimate the pH at the interface and thus the difference in Gibbs free energy and nucleation rate for the formation of the crystalline calcium phosphate species. Although the model relies on fundamental principles and does not consider the formation of other calcium phosphate phases such as ACP and CDA, it could still provide some insights on the composition of these coatings. For example, in Figure 1 it can be observed that the precipitation of DCPD is the fastest when comparing the nucleation rates, but the  $\Delta G$  for its formation becomes positive at high currents. Therefore, DCPD will be the most favourable phase formed at low currents and short deposition times, but might not form at all in other conditions. Finally, another important consequence is that the nucleation rate of OCP is higher than HA at any current. Because of this, the precipitation of OCP will always occur before HA, suggesting that obtaining a coating with pure HA might not be a possibility.

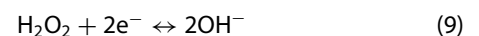
## Electrolyte composition

The vast majority of electrolytes operates in slightly acidic pH condition, typically between 4 and 5. The choice of pH is a delicate balance between an environment too acidic, where the condition for calcium phosphate precipitation will never be met and an environment too alkaline, where undesired precipitation in solution might occur. The preferred  $\text{Ca}^{2+}$  precursor salt is calcium nitrate (often in its tetrahydrate form), with the reason being that the  $\text{NO}_3^-$  ions themselves can undergo electrochemical reduction at the cathode surface, contributing to the increase in pH necessary for phosphate precipitation<sup>36</sup>:



Reaction 7 is especially desirable because, unlike hydrogen evolution, it leads to pH increase without gas formation, which is often responsible for defects in the coating. Phosphate ions on the other hand, are typically introduced as dihydrogen phosphate salts, such as  $\text{NH}_4(\text{H}_2\text{PO}_4)$  or  $\text{NaH}_2\text{PO}_4$ . In most cases, the Ca/P ratio of the precursors is fixed at 1.67. This ratio is specifically chosen to match the ratio in HA and thus promote its precipitation. Besides the Ca and P precursors, other additives are also present.

Hydrogen peroxide is possibly the most common additive found in formulations for electrochemical calcium phosphate deposition. In the deposition process,  $\text{H}_2\text{O}_2$  actually plays a role quite similar to nitrate ions. In fact, it can be reduced in  $\text{OH}^-$  ions at higher potential than water and the reaction does not involve  $\text{H}_2$  gas production<sup>37</sup>:



For this reason, hydrogen peroxide is often added in concentrations up to 9% v/v. At the same time, an excessive concentration of  $\text{H}_2\text{O}_2$  is detrimental, as the rate of  $\text{OH}^-$  production exceeds the rate of consumption during

**Table 1.** Main phases produced during electrochemical deposition, along with their solubility. Data taken from ref.<sup>31</sup>

Compound	Abbr.	Chemical Formula	Ca/P ratio	Solubility at 25°C [-log (K <sub>s</sub> )]
Dicalcium phosphate dihydrate	DCPD	CaHPO <sub>4</sub> ·2H <sub>2</sub> O	1.00	6.6
Octacalcium phosphate	OCP	Ca <sub>8</sub> (HPO <sub>4</sub> ) <sub>2</sub> (PO <sub>4</sub> ) <sub>4</sub> ·5H <sub>2</sub> O	1.33	96.6
Calcium-deficient apatite	CDA	Ca <sub>10-x</sub> (HPO <sub>4</sub> ) <sub>x</sub> (PO <sub>4</sub> ) <sub>6-x</sub> (OH) <sub>2-x</sub>	1.34–1.66	85.1
Hydroxyapatite	HA	Ca <sub>10</sub> (PO <sub>4</sub> ) <sub>6</sub> (OH) <sub>2</sub>	1.67	116.8
Amorphous calcium phosphate	ACP	Ca <sub>x</sub> H <sub>y</sub> (PO <sub>4</sub> ) <sub>z</sub> ·nH <sub>2</sub> O	1.2–2.2	25.7–32.7

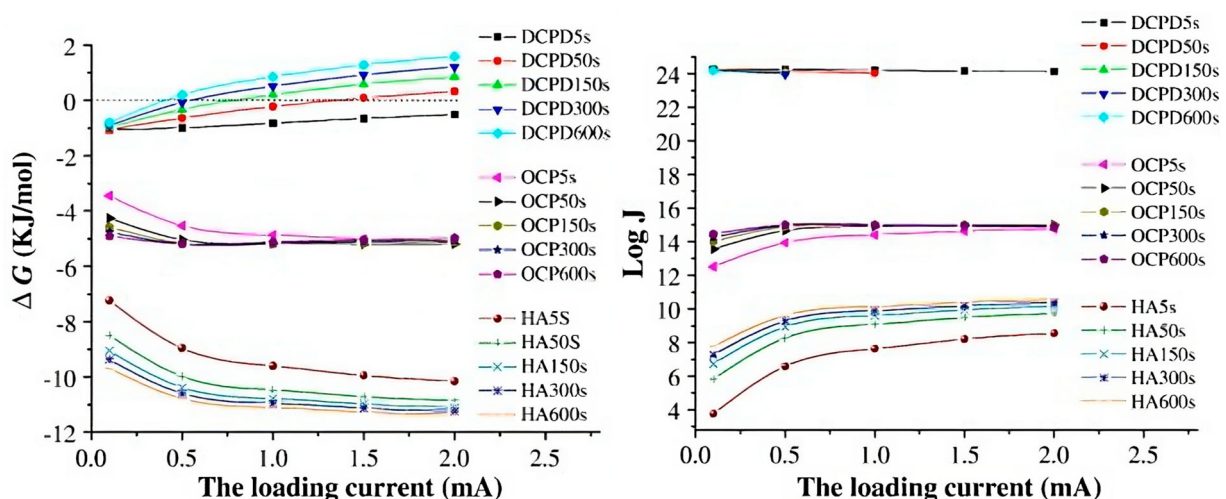
phosphate precipitation, leading to the formation of loosely attached coatings.<sup>37,38</sup> The addition of H<sub>2</sub>O<sub>2</sub> enables the possibility of working at higher current densities without excessive formation of gas bubbles; as a consequence, the composition of the resulting coatings will be improved. For example, T. Mokabber *et al.*<sup>39</sup> discovered that by introducing up to 1.5 wt-% of H<sub>2</sub>O<sub>2</sub> in an electrolyte for constant potential deposition, it is possible to suppress entirely the formation of DCPD, while favouring the formation of OCP and HA. In fact, by working at higher currents the pH at the cathode interface can increase further, shifting the equilibria of the phosphate species from HPO<sub>4</sub><sup>2-</sup> to PO<sub>4</sub><sup>3-</sup>, a result that agrees with the model described in the previous section.

Introduction of secondary ions has been proposed as a way to enhance calcium phosphate coatings properties. These ions are introduced in small quantities, in order to substitute the calcium and phosphate ions present in the lattice without the formation of new phases. Among all calcium phosphate phases, hydroxyapatite has received significant attention as it can incorporate a wide variety of cations and anions. In fact, the composition of the human bone mineral itself includes several ions as substitutes, with the most prominent one being the carbonate ion (CO<sub>3</sub><sup>2-</sup>).<sup>31,32</sup> In this regard, electrochemical deposition has proved to be one of the best techniques for ion substitution, as the only additional step is the inclusion of the secondary ions' precursor salts in the electrolyte formulation. In fact, substitution with multiple secondary ions in the same formulation has already been explored.<sup>40,41</sup>

Introduction of strontium ions has been reported as a viable strategy to enhance biological properties of calcium phosphate coatings.<sup>42,43</sup> The release of Sr<sup>2+</sup> ions from substituted hydroxyapatite stimulates cell proliferation and osteoblastic activity, while also inhibiting osteoclastic bone resorption.<sup>44</sup> Osteoblasts and osteoclasts are cells responsible

for bone tissue formation and degradation respectively. Under normal circumstances, the two types of cells cooperate, ensuring periodic renewal of bone tissue; however, in the case of bone repair it is preferable to offset the activities of the two, with the overall effect being favouring bone regrowth. Finally, the presence of Sr in the hydroxyapatite lattice changes the morphology of the coating, favouring needle-like crystals over the most common plate-like ones as can be seen in Figure 2. Silver,<sup>45–47</sup> zinc<sup>41,48,49</sup> and copper<sup>50,51</sup> ions on the other hand have frequently been explored to provide antibacterial properties to the calcium phosphate coatings. Ensuring that the coatings have good antibacterial properties while maintaining every other biological function intact would drastically reduce the risk of infection during and after surgeries. These elements are ordinarily introduced in small amounts, as they can become cytotoxic in high concentrations, with silver being the most dangerous of the three.<sup>52</sup> In addition to the antibacterial properties, the presence of Zn<sup>2+</sup> is also correlated to improvement in bone tissue healing.<sup>53</sup> Magnesium is another element that is naturally occurring in human bone mineral and whose presence in HA coatings has proved to be beneficial.<sup>54</sup> In fact, magnesium can significantly improve cell adhesion by interacting with osteoblast integrin, a receptor that mediates cell-surface interactions.<sup>55</sup> Interestingly, due to the difference between Mg<sup>2+</sup> and Ca<sup>2+</sup> ions radii (about 0.28 Å), the introduction of magnesium in HA leads to distortions of the lattice, which ultimately end up increasing its solubility.<sup>56</sup>

Conversely, the presence of fluoride ions replacing the hydroxide ions in HA leads to lower solubility of the coating, which makes it particularly helpful when dealing with biodegradable alloys.<sup>57,58</sup> Furthermore, fluoridated calcium phases also exhibit improved osteoblast differentiation, while suppressing osteoclast activity.<sup>59,60</sup>

**Figure 1.**  $\Delta G$  (left) and nucleation rate (right) for DCPD, OCP and HA as a function of the cathodic current. Adapted from ref.<sup>35</sup> with permission from Elsevier.

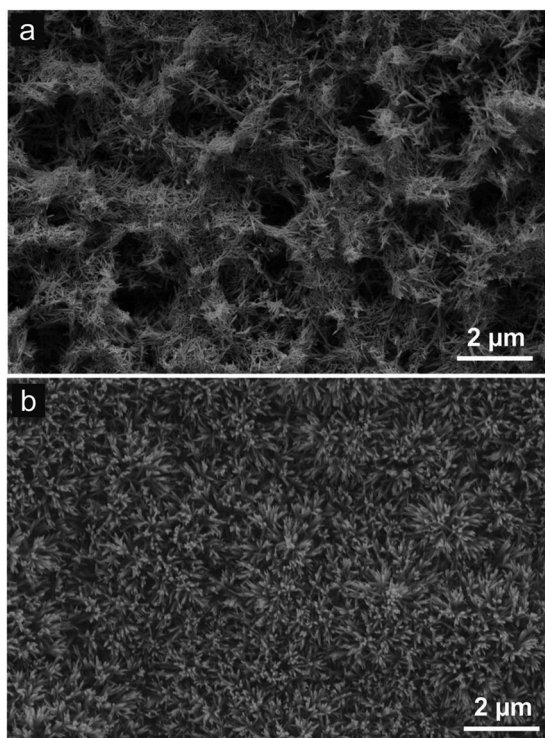


**Figure 2.** Morphology of Sr-substituted hydroxyapatite coatings, with 10% Sr substitution (a) and 50% Sr substitution (b). Adapted from ref.<sup>42</sup> with permission from Elsevier.

### The advantages of pulsed deposition

By providing a pulsed input, whether it's current or voltage, rather than a continuous one, it's possible to solve the major shortcomings of electrochemical deposition, as well as opening up additional possibilities. In fact, the application of pulsed current is already a well-established technique for electroplating at the industrial scale because of the advantages it provides.<sup>61</sup> Optimisation of pulsed deposition protocols is often more challenging than continuous current deposition because of the additional parameters that define the impulse. **Figure 3** highlights the differences between a continuous and a pulsed deposition protocol. Aside from temperature, electrolyte composition and stirring, the only parameters to set for a continuous deposition are the current ( $j$ ) or voltage ( $V$ ) and the total duration ( $t_{TOT}$ ) of the process. On the other hand, a pulsed deposition process is defined by the duration of the 'on-time' of the pulse ( $t_{ON}$ ), the current ( $j_{ON}$ ) or voltage ( $V_{ON}$ ) during  $t_{ON}$ , the duration of

the break time ( $t_{OFF}$ ), as well as the total duration of the deposition,  $t_{TOT}$ . In most cases  $t_{ON}$  and  $t_{OFF}$  are in the range of seconds or even milliseconds, but for calcium phosphate pulsed electrodeposition it's not uncommon to extend these durations to minutes. Moreover, the current ( $j_{OFF}$ ) or voltage ( $V_{OFF}$ ) during the break time are often set to 0, but it is also possible to reverse the polarisation during the break time, giving rise to the pulsed reverse deposition method.

The first main advantage of the pulsed protocol is the reduction in hydrogen bubbles formation during deposition. As previously mentioned, the cathodic polarisation used in electrochemical deposition promotes hydrogen evolution according to reactions 4 and 5. Although this reaction is fundamental for the deposition of the calcium phosphate coatings, an excessive production of  $H_2$  leads to bubble formation. These bubbles can stick to the surface of the coating during the deposition, leaving crater-like defects in their place.<sup>62</sup> When using pulsed deposition, however, the break time allows for the hydrogen bubbles to leave the surface rather than coalesce and grow in size, thus the defectivity of the coatings is significantly reduced.<sup>38</sup> Additionally, when using the pulsed reverse method, the change in polarisation during the break time allows for desorption of adsorbed hydrogen on the active sites of the cathode surface.<sup>63</sup> One clear example of improvement in coating defectivity is shown in **Figure 4**.

The advantages associated with reduced  $H_2$  formation are not simply limited to the reduced coating defectivity; hydrogen evolution poses a strict limitation on the maximum current density that can be used in the deposition. As stated previously, the current density directly influences the phases obtained and the formation of hydroxyapatite, which is often the most desirable calcium phosphate phase, becomes favourable only at high current densities. Therefore, a constraint in the current density will automatically lead to formation of DCPD and OCP phases in the coating. Although these phases can still be converted in HA and  $\beta$ -tricalcium phosphate by heat treatment or alkaline conversion,<sup>64</sup> the final average Ca/P ratio will always remain below 1.67. By reducing the extent of  $H_2$  formation through pulsed current, it's therefore possible to increase the maximum current density  $j_{ON}$  without formation of defects in the coating and increase the Ca/P ratio as a consequence.<sup>37</sup>

Although many electrolyte formulations are explicitly designed with a fixed Ca/P ratio in mind, the concentration

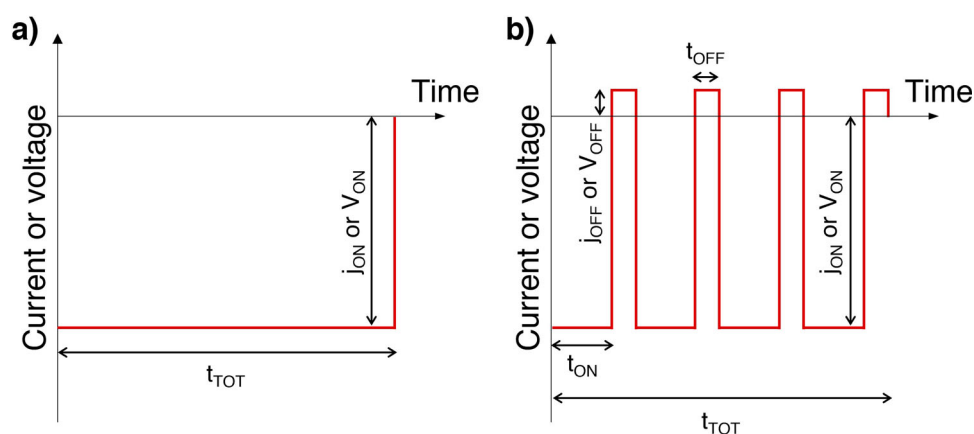


**Figure 3.** Current or voltage profile over time during continuous deposition (a) or pulsed deposition (b).

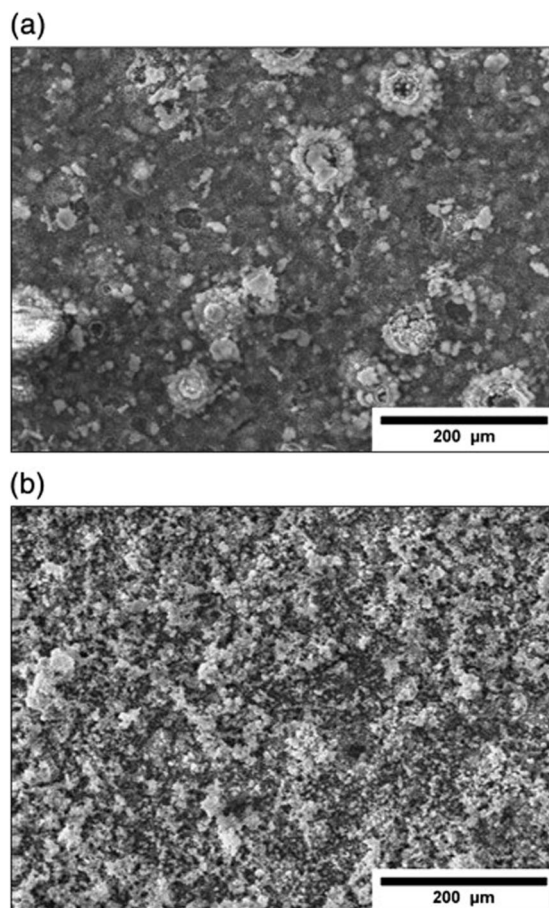


**Figure 4.** Calcium phosphate coatings obtained with constant current deposition (a) and pulsed current deposition (b). The average current density was kept constant in both experiments at  $5 \text{ mA cm}^{-2}$ . Reprinted from ref. <sup>37</sup> with permission from Elsevier.

of the electrolyte at the cathode surface will never coincide with the concentration of the bulk solution. As ions are consumed at the surface to form the calcium phosphate coating, they need to be replenished with ions moving from the solution to the cathode surface. This transport of ions towards the cathode surface is mediated by diffusion and leads to the formation of concentration gradients.<sup>65</sup> As different ions like  $\text{Ca}^{2+}$  and  $\text{HPO}_4^{2-}$  possess different diffusion constants, it is expected that their concentration gradients will not be the same; consequently, the Ca/P ratio at the cathode interface will differ from the bulk Ca/P ratio. In addition to this, calcium ions are positively charged and when placed in an electric field, they will travel towards the region at lower potential, i.e. the cathode; conversely, phosphate species are negatively charged and will move in the opposite direction. Overall, this asymmetry contributes to the concentration imbalance at the cathode surface. During the break time in pulsed electrodeposition, however, the concentration gradients can relax, and the electrolyte can homogenise. The net consequence is that, on average, the deposition occurs with concentrations at the interface that are closer to the nominal concentration when employing pulsed deposition methods, ensuring better composition control. Finally, the ion replenishment during the break time also ensures that the effect of mass transport can be severely reduced or even completely neglected.<sup>66</sup> This translates in the formation of denser coatings, with improved morphology and smaller grain size, which in turn exhibit superior mechanical performances and corrosion resistance.<sup>67,68</sup>

## Conclusions

In summary, electrochemical deposition has proved to be a highly effective method for the synthesis of calcium phosphate coatings for medical applications. The coatings produced with electrochemical deposition feature desirable properties such as good adhesion, compositional homogeneity, and excellent biocompatibility. The low cost and extraordinary versatility of the technique could soon make electrochemical deposition a viable alternative to plasma spraying. Moreover, the major shortcomings of the continuous current method can be easily overcome with the adoption of the pulsed deposition method. In fact, coatings produced with pulsed electrochemical deposition have proved to have lower defects, better composition control and improved morphology.

## Acknowledgements

Paper based on a presentation given at the EDNANO14 and 10th European Pulse Plating Seminar, the latter hosted by EAST Forum, 9–10 June 2022, Kraków, Poland.

## Disclosure statement

No potential conflict of interest was reported by the author(s).

## ORCID

F. Lissandrello  <http://orcid.org/0000-0002-7173-0997>

L. Magagnin  <http://orcid.org/0000-0001-5553-6441>

## References

1. D. F. Williams: *Bioact. Mater.*, **2022**, **10**, 306–322.
2. S. B. Goodman, Z. Yao, M. Keeney and F. Yang: *Biomaterials*, **2013**, **34**, 3174–3183.
3. D. Losic: *Expert Opin. Drug Deliv.*, **2021**, **18**, 1355–1378.
4. A.-M. Zhang, P. Lenin, R.-C. Zeng and M. B. Kannan: *J. Magnes. Alloy.*, **2022**, **10**, 1154–1170.
5. P. Wan, X. Qiu, L. Tan, X. Fan and K. Yang: *Ceram. Int.*, **2015**, **41**, 787–796.
6. B. Wang, Y. Li, S. Wang, F. Jia, A. Bian, K. Wang, L. Xie, K. Yan, H. Qiao, H. Lin, J. Lan, et al.: *Mater. Sci. Eng. C*, **2021**, **129**, 112387.
7. H. Li, Y. Zheng and X. Ji: *J. Mater. Sci. Technol.*, **2023**, **141**, 124–134.
8. N. Mohd Daud, N. B. Sing, A. H. Yusop, F. A. Abdul Majid and H. Hermawan: *J. Orthop. Transl.*, **2014**, **2**, 177–184.
9. H. Chen, E. Zhang and K. Yang: *Mater. Sci. Eng. C*, **2014**, **34**, 201–206.
10. A. Civantos, E. Martinez-Campos, V. Ramos, C. Alvarez, A. Gallardo and A. Abarrategi: *ACS Biomater. Sci. Eng.*, **2017**, **3**, 1245–1261.
11. K. Soballe, E. S. Hansen, H. Brockstedt-Rasmussen and C. Bunger: *J. Bone Jt. Surg. Ser. B.*, **1993**, **75**, 270–278.
12. R. Drevet and H. Benhayoune: *Coatings*, **2022**, **12**, 539.
13. S. Shadanbaz and G. J. Dias: *Acta Biomater.*, **2012**, **8**, 20–30.
14. M. Chambard, O. Marsan, C. Charvillat, D. Grossin, P. Fort, C. Rey, F. Gitzhofer and G. Bertrand: *Surf. Coatings Technol.*, **2019**, **371**, 68–77.
15. R. B. Heimann: *Surf. Coatings Technol.*, **2006**, **201**, 2012–2019.
16. D. Gopi, J. Indira and L. Kavitha: *Surf. Coatings Technol.*, **2012**, **206**, 2859–2869.
17. V. F. Pichugin, R. A. Surmenev, E. V. Shesterikov, M. A. Ryabtseva, E. V. Eshenko, S. I. Tverdokhlebov, O. Prymak and M. Epple: *Surf. Coatings Technol.*, **2008**, **202**, 3913–3920.
18. M. Qadir, Y. Li and C. Wen: *Acta Biomater.*, **2019**, **89**, 14–32.
19. N. Jmal and J. Bouaziz: *Mater. Sci. Eng. C.*, **2017**, **71**, 279–288.
20. J. Chen, Y. Wang, X. Chen, L. Ren, C. Lai, W. He and Q. Zhang: *Mater. Lett.*, **2011**, **65**, 1923–1926.
21. Y. Su, Y. Guo, Z. Huang, Z. Zhang, G. Li, J. Lian and L. Ren: *Surf. Coatings Technol.*, **2016**, **307**, 99–108.
22. X. B. Chen, N. Birbilis and T. B. Abbott: *Corros. Sci.*, **2012**, **55**, 226–232.
23. B. Liu, X. Zhang, G. Y. Xiao and Y. P. Lu: *Mater. Sci. Eng. C.*, **2015**, **47**, 97–104.

24. L. Duta: *Coatings*, **2021**, **11**, 99.
25. M. Djošić, A. Janković and V. Mišković-Stanković: *Materials*, **2021**, **14**, 5391.
26. R. Manoj Kumar, K. K. Kuntal, S. Singh, P. Gupta, B. Bhushan, P. Gopinath and D. Lahiri: *Surf. Coatings Technol.*, **2016**, **287**, 82–92.
27. L. Mohan, D. Durgalakshmi, M. Geetha, T. S. N. Sankara Narayanan and R. Asokamani: *Ceram. Int.*, **2012**, **38**, 3435–3443.
28. M. S. Safavi, F. C. Walsh, M. A. Surmeneva, R. A. Surmenev and J. Khalil-Allafi: *Coatings*, **2021**, **11**, 1–62.
29. T.-T. Li, L. Ling, M.-C. Lin, H.-K. Peng, H.-T. Ren, C.-W. Lou and J.-H. Lin: *J. Mater. Sci.*, **2020**, **55**, 6352–6374.
30. K. J. Powell, P. L. Brown, R. H. Byrne, T. Gajda, G. Hefter, S. Sjöberg and H. Wanner: *Pure Appl. Chem.*, **2005**, **77**, 739–800.
31. S. V. Dorozhkin: *Materials*, **2009**, **2**, 399–498.
32. S. Von Euw, Y. Wang, G. Laurent, C. Drouet, F. Babonneau, N. Nassif and T. Azais: *Sci. Rep.*, **2019**, **9**, 1–11.
33. S. Danti, et al.: *J. Funct. Biomater.*, **2022**, **13**, 65.
34. O. Suzuki, Y. Shiwaku and R. Hamai: *Dent. Mater. J.*, **2020**, **39**, 187–199.
35. S. Chen, W. Liu, Z. Huang, X. Liu, Q. Zhang and X. Lu: *Mater. Sci. Eng. C*, **2009**, **29**, 108–114.
36. D. Zimmermann, A. G. Muñoz and J. W. Schultze: *Electrochim. Acta*, **2003**, **48**, 3267–3277.
37. R. Drevet, H. Benhayoune, L. Wortham, S. Potiron, J. Douglade and D. Laurent-Maquin: *Mater. Charact.*, **2010**, **61**, 786–795.
38. H. Benhayoune, R. Drevet, J. Fauré, S. Potiron, T. Gloriant, H. Oudadesse and D. Laurent-Maquin: *Adv. Eng. Mater.*, **2010**, **12**, B192–B199.
39. T. Mokabber, L. Q. Lu, P. van Rijn, A. I. Vakis and Y. T. Pei: *Surf. Coatings Technol.*, **2018**, **334**, 526–535.
40. L. Morejón-Alonso, C. Mochales, L. Nascimento and W. D. Müller: *Mater. Lett.*, **2019**, **248**, 65–68.
41. D. Gopi, A. Karthika, S. Nithiya and L. Kavitha: *Mater. Chem. Phys.*, **2014**, **144**, 75–85.
42. R. Schmidt, A. Gebert, M. Schumacher, V. Hoffmann, A. Voss, S. Pilz, M. Uhlemann, A. Lode and M. Gelinsky: *Mater. Sci. Eng. C*, **2020**, **108**, 110425.
43. R. Drevet and H. Benhayoune: *Mater. Sci. Eng. C*, **2013**, **33**, 4260–4265.
44. X. Cui, et al.: *Bioact. Mater.*, **2020**, **5**, 334–347.
45. Y. Yan, X. Zhang, Y. Huang, Q. Ding and X. Pang: *Appl. Surf. Sci.*, **2014**, **314**, 348–357.
46. T. Mokabber, H. T. Cao, N. Norouzi, P. Van Rijn and Y. T. Pei: *ACS Appl. Mater. Interfaces*, **2020**, **12**, 5531–5541.
47. M. Furko and C. Balázi: *Materials*, **2020**, **13**, 4690.
48. D. M. Vranceanu, E. Ungureanu, I. C. Ionescu, A. C. Parau, A. E. Kiss, A. Vladescu and C. M. Cotrut: *Coatings*, **2022**, **12**, 69.
49. Q. Ding, X. Zhang, Y. Huang, Y. Yan and X. Pang: *J. Mater. Sci.*, **2015**, **50**, 189–202.
50. Y. Huang, X. Zhang, R. Zhao, H. Mao, Y. Yan and X. Pang: *J. Mater. Sci.*, **2015**, **50**, 1688–1700.
51. C. Wolf-Brandstetter, S. Oswald, S. Bierbaum, H.-P. Wiesmann and D. Scharnweber: *J. Biomed. Mater. Res. Part B Appl. Biomater.*, **2014**, **102**, 160–172.
52. O. Bondarenko, K. Juganson, A. Ivask, K. Kasemets, M. Mortimer and A. Kahru: *Arch. Toxicol.*, **2013**, **87**, 1181–1200.
53. J. P. O'Connor, D. Kanjilal, M. Teitelbaum, S. S. Lin and J. A. Cottrell: *Materials*, **2020**, **13**, 2211.
54. S. F. Zhao, Q. H. Jiang, S. Peel, X. X. Wang and F. M. He: *Clin. Oral Implants Res.*, **2013**, **24**, 34–41.
55. H. Zreiqat, C. R. Howlett, A. Zannettino, P. Evans, G. Schulze-Tanzil, C. Knabe and M. Shakibaei: *J. Biomed. Mater. Res.*, **2002**, **62**, 175–184.
56. D. M. Vranceanu, I. C. Ionescu, E. Ungureanu, M. O. Cojocaru, A. Vladescu and C. M. Cotrut: *Coatings*, **2020**, **10**, 727.
57. E. C. Meng, et al.: *Appl. Surf. Sci.*, **2011**, **257**, 4811–4816.
58. J. Wang, Y. Chao, Q. Wan, Z. Zhu and H. Yu: *Acta Biomater.*, **2009**, **5**, 1798–1807.
59. H. Qu and M. Wei: *Acta Biomater.*, **2006**, **2**, 113–119.
60. J. Sun, T. Wu, Q. Fan, Q. Hu and B. Shi: *RSC Adv.*, **2019**, **9**, 16106–16118.
61. C. Larson and J. P. G. Farr: *Trans. IMF*, **2012**, **90**, 20–29.
62. A. Mehrvarz, Y. Ghazanfar-Ahari, J. Khalil-Allafi, S. Mahdavi and M. Etminanfar: *Ceram. Int.*, **2022**, **48**, 2191–2202.
63. E. Vidal, et al.: *Surf. Coatings Technol.*, **2019**, **358**, 266–275.
64. R. Štulajterová and L. Medvecký: *Colloids Surf. A Physicochem. Eng. Asp.*, **2008**, **316**, 104–109.
65. A. J. Bard, L. R. Faulkner and H. S. White: 'Electrochemical methods: fundamentals and applications', **2022**; New York, John Wiley & Sons, Inc.
66. D. J. Blackwood and K. H. W. Seah: *Mater. Sci. Eng. C*, **2010**, **30**, 561–565.
67. M. B. Kannan and O. Wallipa: *Mater. Sci. Eng. C*, **2013**, **33**, 675–679.
68. P. Peng, S. Kumar, N. H. Voelcker, E. Szili, R. S. C. Smart and H. J. Griesser: *J. Biomed. Mater. Res. Part A*, **2006**, **76A**, 347–355.